THE JOURNAL OF BIOLOGICAL CHEMISTRY VOL. 286, NO. 23, pp. 20625–20636, June 10, 2011

Identification of Critical Residues in $G\alpha_{13}$ for Stimulation of p115RhoGEF Activity and the Structure of the $G\alpha_{13}$-p115RhoGEF Regulator of G Protein Signaling Homology (RH) Domain Complex*[S]

Received for publication, November 10, 2010, and in revised form, April 8, 2011 Published, JBC Papers in Press, April 20, 2011, DOI 10.1074/jbc.M110.201392

Nicole Hajicek[‡§], Mutsuko Kukimoto-Niino[¶], Chiemi Mishima-Tsumagari[¶], Christina R. Chow[‡], Mikako Shirouzu[¶], Takaho Terada[¶], Maulik Patel[‡], Shigeyuki Yokoyama[¶‖], and Tohru Kozasa[‡§¶1]

From the [‡]Department of Pharmacology, College of Medicine, University of Illinois, Chicago, Illinois 60612, the [¶]RIKEN Systems and Structural Biology Center, 1-7-22 Suehiro-cho, Tsurumi, Yokohama 230-0045, Japan, the [‖]Department of Biophysics and Biochemistry, Graduate School of Science, University of Tokyo, 7-3-1 Hongo, Bunkyo-ku, Tokyo 113-0033, Japan, and the [§]Laboratory of Systems Biology and Medicine, Research Center for Advanced Science and Technology, University of Tokyo, 4-6-1 Komaba, Meguro-ku, Tokyo 153-8904, Japan

RH-RhoGEFs are a family of guanine nucleotide exchange factors that contain a regulator of G protein signaling homology (RH) domain. The heterotrimeric G protein $G\alpha_{13}$ stimulates the guanine nucleotide exchange factor (GEF) activity of RH-RhoGEFs, leading to activation of RhoA. The mechanism by which $G\alpha_{13}$ stimulates the GEF activity of RH-RhoGEFs, such as p115RhoGEF, has not yet been fully elucidated. Here, specific residues in $G\alpha_{13}$ that mediate activation of p115RhoGEF are identified. Mutation of these residues significantly impairs binding of $G\alpha_{13}$ to p115RhoGEF as well as stimulation of GEF activity. These data suggest that the exchange activity of p115RhoGEF is stimulated allosterically by $G\alpha_{13}$ and not through its interaction with a secondary binding site. A crystal structure of $G\alpha_{13}$ bound to the RH domain of p115RhoGEF is also presented, which differs from a previously crystallized complex with a $G\alpha_{13}$-$G\alpha_{i1}$ chimera. Taken together, these data provide new insight into the mechanism by which p115RhoGEF is activated by $G\alpha_{13}$.

Heterotrimeric guanine nucleotide binding proteins (G proteins), composed of α, β, and γ subunits, act as molecular switches that cycle between an inactive, GDP-bound state and an active, GTP-bound state upon stimulation of G protein-coupled receptors (1). Once activated, the GTP-bound $G\alpha$ subunit dissociates from the $G\beta\gamma$ dimer, both of which regulate the activity of multiple intracellular effectors to elicit cellular responses. The duration of signaling mediated by $G\alpha$ is dictated by the lifetime of bound GTP. All $G\alpha$ subunits have intrinsic GTPase activity that hydrolyzes GTP to GDP, and this rate of hydrolysis is enhanced by GAPs,[2] such as RGS proteins (2), which bind the switch regions of activated $G\alpha$ subunits, stabilize the transition state for GTP hydrolysis, and thus accelerate the hydrolysis of GTP to GDP (3, 4). Once in the GDP-bound state, $G\alpha$ subunits reassociate with $G\beta\gamma$ and are capable of initiating another round of signaling.

$G\alpha_{13}$ is one of two members of the G_{12} family of G proteins (5) and has been implicated in regulating multiple cellular processes that depend on activation of the monomeric GTPase RhoA, including gene transcription, embryogenesis, and rearrangement of the actin cytoskeleton (6–8). A direct link between $G\alpha_{13}$ and RhoA was established with the discovery of p115RhoGEF, the founding member of a family of RhoA-specific GEFs containing an RH domain in their N termini (RH-RhoGEFs) (9). Together with p115RhoGEF, PDZ-RhoGEF and LARG constitute the RH-RhoGEF family in mammals (10, 11). The RH domain of p115RhoGEF has low sequence similarity to canonical RGS proteins but nevertheless functions as a GAP for $G\alpha_{13}$ (12). Although the structure of the RH domain of p115RhoGEF is similar to that of other RGS proteins (13), additional elements flanking the RGS box are required for GAP activity (14) and stability of the isolated domain (15). In addition to its RH domain, p115RhoGEF also contains the tandem DH/PH domains characteristic of Dbl family RhoGEFs. The nucleotide exchange activity of p115RhoGEF can be directly stimulated by $G\alpha_{13}$ *in vitro* (9), and $G\alpha_{13}$ acts synergistically

* This work was supported, in whole or in part, by National Institutes of Health Grants GM61454 and GM074001 (to T. K.). This work was also supported by a grant-in-aid from the Greater Midwest Affiliate of the American Heart Association (to T. K.), the Targeted Proteins Research Program (TPRP) from the Ministry of Education, Culture, Sports, Science and Technology of Japan; the Funding Program for World-Leading Innovative R&D on Science and Technology from the Japan Society for the Promotion of Science; a predoctoral fellowship from the Greater Midwest Affiliate of the American Heart Association (to N. H.); and the Japan Society for the Promotion of Science (to N. H.).

[S] The on-line version of this article (available at http://www.jbc.org) contains supplemental Figs. 1–3 and Tables 1–3.

The atomic coordinates and structure factors (code 3AB3) have been deposited in the Protein Data Bank, Research Collaboratory for Structural Bioinformatics, Rutgers University, New Brunswick, NJ (http://www.rcsb.org/).

[1] To whom correspondence should be addressed: Laboratory of Systems Biology and Medicine, Research Center for Advanced Science and Technology, University of Tokyo, 4-6-1 Komaba, Meguro-ku, Tokyo 153-8904, Japan. Tel.: 81-3-5452-5359; Fax: 81-3-5452-5231; E-mail: kozasa@lsbm.org.

[2] The abbreviations used are: GAP, GTPase-activating protein; DH, Dbl homology; GEF, guanine nucleotide exchange factor; GTPγS, guanosine 5′-3-*O*-(thio)triphosphate; LARG, leukemia-associated RhoGEF; PDZ, post-synaptic density protein 95, discs large, zonula occludens; PH, pleckstrin homology; RGS, regulator of G protein signaling; RH, RGS homology; Sf9, *Spodoptera frugiperda*; SRE, serum response element; TEV, tobacco etch virus; TLCK, N^{α}-tosyl-L-lysine chloromethyl ketone; TPCK, *N*-*p*-tosyl-L-phenylalanine chloromethyl ketone.

with p115RhoGEF to activate Rho-dependent signaling in cells (16). Thus, p115RhoGEF functions as both an effector and a GAP for $G\alpha_{13}$. Although the relationship between p115RhoGEF and $G\alpha_{13}$ has been well established, the precise mechanism by which $G\alpha_{13}$ regulates the activity of p115RhoGEF remains to be fully elucidated.

The molecular mechanisms regulating p115RhoGEF activity are likely to be complex and may involve multiple intermolecular interfaces with $G\alpha_{13}$. It has been clearly demonstrated that $G\alpha_{13}$ binds directly to the RH domain of p115RhoGEF (12, 15). Furthermore, this domain is required for both basal and $G\alpha_{13}$-stimulated nucleotide exchange activity, suggesting that it plays a critical role in the activation mechanism (15). A structure of the RH domain of p115RhoGEF bound to an AlF_4^--activated $G\alpha_{13}$-$G\alpha_{i1}$ chimera has been solved by x-ray crystallography and revealed that the α subunit engages this domain through two distinct interfaces (17). In addition to interacting with switch regions I and II of $G\alpha_{13/i1}$ through an N-terminal extension of the RGS box, the RH domain also docks into the hydrophobic groove between the α_2 and α_3 helices of $G\alpha_{13/i1}$, a highly conserved effector interface among other Gα-effector pairs (18–21). However, many of the residues in the α_3 helix of this chimera are derived from $G\alpha_{i1}$, and its ability to activate p115RhoGEF has not been clearly demonstrated. Thus, the role of residues in the α_3 helix in regulating p115RhoGEF activity is unknown. $G\alpha_{13}$ has also been reported to bind to the isolated DH/PH domains of p115RhoGEF *in vitro* (15); however, it has no capacity to directly stimulate the GEF activity of this fragment. Therefore, the role of additional binding sites outside of the RH domain is also unclear.

Here, specific residues in $G\alpha_{13}$ that mediate activation of p115RhoGEF are identified. We demonstrate that mutation of these residues, which bind to the RH domain of p115RhoGEF, significantly impairs binding of $G\alpha_{13}$ to p115RhoGEF as well as stimulation of GEF activity in cells and *in vitro*. Our results suggest that the initial step in stimulation of exchange activity by $G\alpha_{13}$ involves allosteric regulation through interaction with the RH domain of p115RhoGEF. We also present a crystal structure of $G\alpha_{13}$ bound to the RH domain of p115RhoGEF, which differs in several respects from the previously crystallized complex using the $G\alpha_{13/i1}$ chimera (17) and reinforces the results of our biochemical analysis. This structure provides a more accurate picture of the $G\alpha_{13}$-p115RhoGEF RH interface, whereas the biochemical data provide new insight into the mechanism by which p115RhoGEF is activated by $G\alpha_{13}$.

EXPERIMENTAL PROCEDURES

Generation of Constructs

$G\alpha_{13}$ Mutants—Single point mutations were introduced into the mammalian expression vector pCMV5 harboring murine $G\alpha_{13}$ Q226L for use in SRE-luciferase assays or the baculovirus transfer vector pFastBac HTa (Invitrogen) encoding $G\alpha_{i/13}$ for protein expression using the QuikChange site-directed mutagenesis kit (Stratagene) according to the manufacturer's protocol. The T274E/N278A double mutant was generated using either pCMV5-$G\alpha_{13}$ Q226L T274E or pFastBac HTa-$G\alpha_{i/13}$ T274E as the template. Sense and antisense primer pairs used to introduce each mutation were as follows: N270A, 5′-CGCCTTACAGAATCTCTGGCCATTTTTG-AAACAATTG and 5′-CAATTGTTTCAAAAATGGCC-AGAGATTCTGTAAGGCG; T274E, 5′-CTGAACAT-TTTTGAAGAGATTGTCAACAATCGGGTTTTCAGC and 5′-GCTGAAAACCCGATTGTTGACAATCTCTTCAAAAA-TGTTCAG; N278A, 5′-GAAACAATTGTCAACGCTCG-GGTTTTCAGCAACG and 5′-CGTTGCTGAAAACCCGA-GCGTTGACAATTGTTTC; T274E/N278A, 5′-GAAGA-GATTGTCAACGCTCGGGTTTTCAGCAACG and 5′-CGT-TGCTGAAAACCCGAGCGTTGACAATCTCTTC. Mutated bases are underlined. Introduction of the desired mutation was verified by automated dideoxy sequencing of each construct.

Full-length $G\alpha_{13}$—Full-length $G\alpha_{13}$ ($G\alpha_{13}$ FL) was generated by first introducing a silent mutation into pCMV5-$G\alpha_{13}$ by QuikChange site-directed mutagenesis that eliminates an internal HindIII site using the primers 5′-GCCCGAGA-GAAGCTCCATATTCCCTGGGG and 5′-CCCCAGGG-AATATGGAGCTTCTCTCGGGC. Mutated bases are underlined. KpnI and HindIII sites were then introduced at the 5′- and 3′-ends, respectively, of $G\alpha_{13}$ by PCR using pCMV5-$G\alpha_{13}$ lacking the internal HindIII site as the template and the primers 5′-GGTACCGCGGACTTCCTGCCGTC and 5′-GACCA-AGCTTTCACTGCAGCATGAGCTG. The PCR products were digested with KpnI and HindIII and ligated into the pFast-Bac HT(−) vector containing the N-terminal α_1 helix of $G\alpha_{i1}$ such that the construct contains, from the N terminus, a His_6 tag, residues 1–28 of $G\alpha_{i1}$, a TEV protease site, and residues 2–377 of $G\alpha_{13}$.

p115RhoGEFΔC—Tyr^{763} of p115RhoGEF was mutated to a stop codon using QuikChange site-directed mutagenesis using pFastBac HTc-p115RhoGEF as the template and the primers 5′-CACTGAGACTGCCGGATAACTGAAAGTCCCTGCCC and 5′-GGGCAGGGACTTTCAGTTATCCGGCAGTCTC-AGTG. Mutated bases are underlined.

Protein Purification

His_6-$G\alpha_{i/13}$ (Wild Type and Mutant)—His_6-$G\alpha_{i/13}$ and His_6-$G\alpha_{i/13}$ harboring the N270A, T274E, N278A, or T274E/N278A mutation(s) were purified from the soluble fraction of Sf9 cells as described previously (22). The His_6 tag was removed for crystallography by incubating His_6-$G\alpha_{i/13}$ with 2% (w/w) His_6-TEV protease overnight at 4 °C. Uncut His_6-$G\alpha_{i/13}$ and His_6-TEV protease were removed using a HisTrap HP column (GE Healthcare Life Sciences). $G\alpha_{i/13}$ was subjected to gel filtration chromatography on a Superdex 200 10/300 size exclusion column (GE Healthcare) and eluted in buffer containing 20 mM HEPES, pH 8.0, 100 mM NaCl, 10 mM 2-mercaptoethanol, 1 mM $MgCl_2$, 10 μM GDP, and 10% glycerol. The protein was aliquoted, snap-frozen in liquid nitrogen, and stored at −80 °C until use.

Full-length $G\alpha_{13}$—His_6-$G\alpha_{i/13}$ FL was purified from Sf9 cells in the same fashion as His_6-$G\alpha_{i/13}$. After elution from nickel-NTA resin (Qiagen), fractions containing His_6-$G\alpha_{i/13}$ FL were pooled and incubated with 2% (w/w) His_6-TEV protease overnight at 4 °C to remove the His_6 tag and α_1 helix of $G\alpha_{i1}$. The protein was concentrated and buffer-exchanged to imidazole-free buffer using an Amicon Ultra 30k centrifugal filter device

(Millipore Corp.). The protein was aliquoted, snap-frozen in liquid nitrogen, and stored at −80 °C until use.

p115RhoGEF—Sf9 cells expressing His_6-p115RhoGEF were resuspended in lysis buffer (20 mM HEPES, pH 8.0, 100 mM NaCl, 10 mM imidazole, 10 mM 2-mercaptoethanol, 16 μg/ml TPCK, TLCK, and PMSF, and 3.2 μg/ml leupeptin and lima bean trypsin inhibitor) and lysed by nitrogen cavitation. The lysate was clarified by centrifugation at 100,000 × *g* for 30 min at 4 °C. The soluble portion of the lysate was diluted 2-fold with lysis buffer and applied to a nickel-NTA column equilibrated with lysis buffer. The column was washed with 20 bed volumes of wash buffer (20 mM HEPES, pH 8.0, 400 mM NaCl, 20 mM imidazole, 10 mM 2-mercaptoethanol, 16 μg/ml TPCK, TLCK, and PMSF, and 3.2 μg/ml leupeptin and lima bean trypsin inhibitor), and bound protein was eluted from the column using elution buffer (20 mM HEPES, pH 8.0, 400 mM NaCl, 300 mM imidazole, 10 mM 2-mercaptoethanol, 16 μg/ml TPCK, TLCK, and PMSF, and 3.2 μg/ml leupeptin and lima bean trypsin inhibitor). Peak fractions containing His_6-p115RhoGEF were pooled and dialyzed overnight at 4 °C against dialysis buffer (20 mM HEPES, pH 8.0, 400 mM NaCl, 10 mM 2-mercaptoethanol) in the presence of 2% (w/w) His_6-TEV protease. The solution was supplemented with 10% glycerol and applied to a HisTrap HP column to remove remaining His_6-p115RhoGEF and His_6-TEV protease. Flow-through fractions were collected and applied to a HiPrep 16/60 Sephacryl S-300 HR column (GE Healthcare) equilibrated in gel filtration buffer (20 mM HEPES, pH 8.0, 150 mM NaCl, 10 mM 2-mercaptoethanol, 10% glycerol). Fractions containing p115RhoGEF were pooled and subjected to further purification on a Superdex 200 HR 10/30 size exclusion column (GE Healthcare) equilibrated in gel filtration buffer. Fractions containing p115RhoGEF were pooled and concentrated using an Amicon Ultra 30k centrifugal filter device. The protein was aliquoted, snap-frozen in liquid nitrogen, and stored at −80 °C until use.

p115RhoGEFΔC—His_6-p115RhoGEFΔC(1–762) was purified from Sf9 cells in the same fashion as full-length p115RhoGEF except that the final round of size exclusion chromatography utilized a HiLoad Superdex 200 16/60 size exclusion column (GE Healthcare), and the protein was eluted in buffer containing 20 mM HEPES, pH 8.0, 100 mM NaCl, 1 mM EDTA, 10% glycerol, and 2 mM DTT. The protein was aliquoted, snap-frozen in liquid nitrogen, and stored at −80 °C until use.

GST-p115RhoGEF RH Domain—The GST-tagged RH domain of p115RhoGEF was purified from *Escherichia coli* as described previously (22).

RhoA—GST-RhoA lacking the C-terminal CAA*X* motif (RhoA(1–181)) was expressed from the plasmid pGEX-6P (GE Healthcare) in the *E. coli* strain BL21-CodonPlus (DE3)-RP (Stratagene). Cells were grown at 30 °C to an A_{600} of 0.6–0.8, and protein expression was induced with 200 μM isopropyl β-D-1-thiogalactopyranoside for 6 h. Cells were resuspended in lysis buffer (50 mM HEPES, pH 7.5, 1 mM EDTA, 1 mM DTT, 200 mM NaCl, 5 mM $MgCl_2$, 10 μM GDP, 10% glycerol) and lysed with lysozyme and sonication. The lysate was clarified by centrifugation at 100,000 × *g* for 30 min at 4 °C. The soluble portion of the lysate was applied to a column of glutathione-Sepharose 4B beads (GE Healthcare) equilibrated with lysis buffer. The column was washed with 10 bed volumes of lysis buffer, followed by 20 bed volumes of cleavage buffer (50 mM Tris, pH 7.5, 1 mM EDTA, 1 mM DTT, 5 mM $MgCl_2$, 10 μM GDP). On-column cleavage of the GST tag was achieved using PreScission protease according to the manufacturer's protocol (GE Healthcare). Cleaved RhoA was eluted from the column using lysis buffer. Fractions containing RhoA were pooled and concentrated using an Amicon Ultra 15k centrifugal filter device. The protein was aliquoted, snap-frozen in liquid nitrogen, and stored at −80 °C until use. To form nucleotide-free RhoA for crystallography, the protein was incubated with an excess of EDTA on ice.

Biochemical Experiments

SRE-luciferase Assays—Assays were performed as described (23), with the following modification. Each well was co-transfected with 200 ng of pGL3-SRE.L, 100 ng of pCMV5-LacZ, and 10 ng of empty pCMV5 vector or the indicated $G\alpha_{13}$ construct using Lipofectamine2000 (Invitrogen). For immunoblotting of cell lysates, samples were harvested directly into SDS-PAGE sample buffer and boiled. Cell lysate was separated by SDS-PAGE, and $G\alpha_{13}$ was detected by Western blotting with the B860 antibody (24). GAPDH was detected using a monoclonal antibody (clone 6C5, Ambion).

In Vitro Trypsin Protection Assays—3 μg of $G\alpha_{i/13}$ protein (wild type or mutant) was diluted into reaction buffer (20 mM HEPES, pH 8.0, 5 mM $MgCl_2$, 100 μM GDP) and incubated on ice for 45 min in the presence or absence of AlF_4^- (10 mM NaF, 30 μM $AlCl_3$). Trypsin was added to a final concentration of 13.3% (w/w), and the samples were incubated at 30 °C for 15 min. The reaction was terminated by the addition of SDS-PAGE sample buffer and boiling.

GST Pull-down Assays—Assays were preformed as described previously (22), with the exception that bound proteins were released from the beads by the addition of SDS-PAGE sample buffer and boiling.

Single Turnover GAP Assays—GTPase assays were performed as described previously (12), except that reactions were incubated on ice. [γ-^{32}P]GTP (specific activity = 6,000 Ci/mmol) was obtained from PerkinElmer Life Sciences.

Gel Filtration of Full-length p115RhoGEF with His_6-$G\alpha_{i/13}$ or His_6-$G\alpha_{i/13}$ T274E/N278A—2.8 nmol of full-length p115RhoGEF were incubated with 5.6 nmol of His_6-$G\alpha_{i/13}$ (wild type or mutant) for 30 min on ice in gel filtration buffer (20 mM HEPES, pH 8.0, 1 mM EDTA, 2 mM DTT, 150 mM NaCl, 5 mM $MgCl_2$, 10 μM GDP) in the presence or absence of AlF_4^- (10 mM NaF, 20 μM $AlCl_3$). The total volume of each sample was 200 μl. The proteins were fractionated at 4 °C on a Superdex 200 HR 10/30 size exclusion column equilibrated in the same buffer as the sample.

In Vitro RhoGEF Assays—Assays were performed as described previously (25). [^{35}S]GTPγS (specific activity = 1,250 Ci/mmol) was obtained from PerkinElmer Life Sciences.

Crystallization and Data Collection

Crystallization—To form the $G\alpha_{i/13}$-p115ΔC-RhoA complex, $G\alpha_{i/13}$ was activated with 8× AlF_4^- (80 mM NaF, 160 μM

$AlCl_3$) on ice for 15 min and mixed with an equimolar amount of p115RhoGEFΔC and nucleotide-free RhoA. The complex was subjected to size exclusion chromatography on a HiLoad Superdex 200 10/16 gel filtration column, and fractions containing the stoichiometric complex were pooled and concentrated using an Amicon4 10k centrifugal filter device. Screening of the Gα$_{i/13}$-p115RhoGEFΔC-RhoA complex was carried out using vapor diffusion at 20 °C. Diffraction quality crystals of the Gα$_{i/13}$-p115RhoGEF RH domain complex were grown against a reservoir solution containing 15% PEG 4000 and 0.1 M HEPES (pH 7.0). Single crystals were coated with the reservoir solution containing 20% PEG 400 as a cryoprotectant, mounted using a nylon loop, and flash-cooled in the cold stream of the goniometer.

Data Collection—Diffraction data were collected at 100 K with a wavelength of 1.0 Å at SPring-8 beam line BL41XU (Harima, Japan). Data were processed with the HKL2000 program (26). The structure of the Gα$_{i/13}$-p115RhoGEF RH domain complex was determined by molecular replacement with the program MOLREP (CCP4), using the RH domain of p115RhoGEF (Protein Data Bank entry 1IAP, chain A) and Gα$_{i/13}$ (Protein Data Bank entry 1ZCB) as search models. The model was corrected iteratively using O (27), and structure refinement was carried out using CNS (Crystallography and NMR System) (28). The final refinement statistics are shown in Table 1. The quality of the model was inspected by the program PROCHECK in the CCP4 suite (29). Structural similarities were calculated with DALI (30). Solvent-accessible surface area was calculated with the program AREALMOL in the CCP4 suite (29). Graphic figures were created with the program PyMOL (31).

RESULTS

Previous studies have suggested that the region of Gα$_{13}$ responsible for stimulating the guanine nucleotide exchange activity of p115RhoGEF is located C-terminal to the three switch regions (23, 32). These results are supported by crystallographic data, which demonstrate that the α_3 helix and α_3-β_5 loop in Gα$_{13}$ form a putative effector binding site with the RH domain of p115RhoGEF (17). However, the capacity of residues in this region to stimulate GEF activity has not been directly demonstrated. We utilized these data along with the interaction between Gα$_q$ and its effectors PLC-β and GRK2 as models in order to identify specific amino acid residues responsible for activating p115RhoGEF. Recent work has identified several residues that are critical for the interaction between Gα$_q$ and these effectors, namely Ala^{253}, Thr^{257}, and Tyr^{261} (20, 33).[3] The Gα$_q$-PLC-β interaction was selected as a model because, like RH-RhoGEFs, PLC-β functions both as a GAP (34) and effector (35) for Gα$_q$. Based on these data, Asn^{270}, Thr^{274}, and Asn^{278} in Gα$_{13}$, which correspond to Ala^{253}, Thr^{257}, and Tyr^{261} in Gα$_q$ (Fig. 1*A*), were targeted for site-directed mutagenesis, and the effects of these mutations on the ability of Gα$_{13}$ to regulate p115RhoGEF activity were examined.

[3] K. Tsuboi and T. Kozasa, unpublished data.

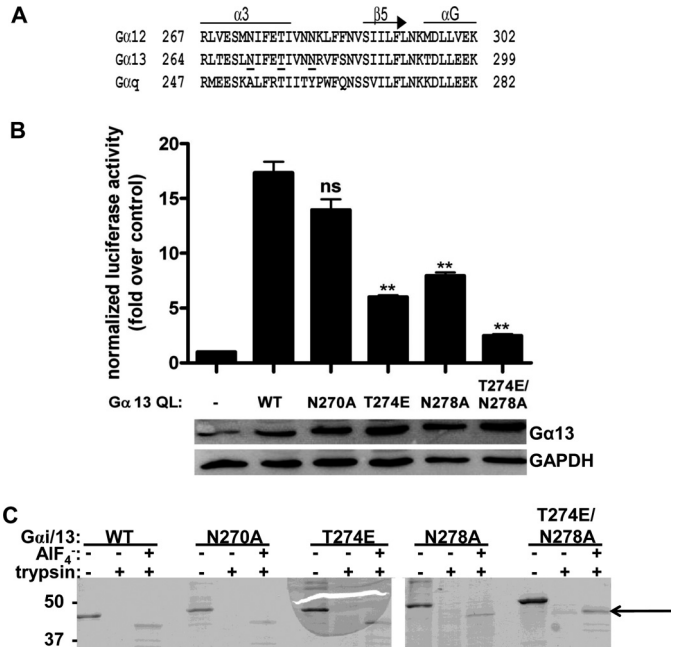

FIGURE 1. **Characterization of Gα$_{i/13}$ mutants.** *A*, a primary sequence alignment of murine Gα$_{12}$, Gα$_{13}$, and Gα$_q$ was generated using the program T-Coffee. Residues in Gα$_{13}$ analyzed by site-directed mutagenesis in this study are *underlined*. Secondary structure was assigned based on the crystal structure of the Gα$_{13/i1}$-p115 RH domain complex (Protein Data Bank entry 1SHZ) (17). *B*, the T274E and N278A mutations in Gα$_{13}$ impair Rho activation in cells. HeLa cells were transiently transfected with empty vector or the indicated Gα$_{13}$ QL construct. The luciferase activity of cell lysates was determined as described under "Experimental Procedures." Total cell lysate was immunoblotted for either Gα$_{13}$ or GAPDH. Data are presented as the mean ± S.E. (*error bars*) of triplicate determinations from a single experiment, representative of three independent experiments with similar results. Data were analyzed by one-way analysis of variance followed by Dunnett's post-test. Statistically significant difference from Gα$_{13}$ QL is shown as follows. *ns*, not significant; **, $p < 0.01$. *C*, Gα$_{i/13}$ mutants can undergo activation-dependent conformational changes. Gα$_{i/13}$ (wild type or mutant) was subjected to limited trypsin digestion in the presence or absence of AlF_4^-. After proteolysis, proteins were separated by SDS-PAGE and stained with Coomassie Brilliant Blue. The primary protected species is indicated with an *arrow*. The positions of molecular mass standards, in kDa, are shown on the *left*.

The T274E and N278A Mutations Impair Rho Activation in Cells—A constitutively active mutant of Gα$_{13}$, Gα$_{13}$ Q226L (hereafter referred to as Gα$_{13}$ QL), has been shown to stimulate transcription from the SRE in a Rho-dependent manner when overexpressed in cells (6). Therefore, to test the ability of the N270A, T274E, N278A, and T274E/N278A mutants to stimulate Rho activation, HeLa cells, which endogenously express RH-RhoGEFs and RhoA, were transiently co-transfected with plasmids encoding each mutant in the background of Gα$_{13}$ QL and a construct encoding the luciferase reporter gene under the control of the SRE. The activation status of Rho in cells was indirectly measured as luciferase activity of cell lysates. In this system, the N270A mutation in Gα$_{13}$ QL did not affect Rho activation compared with Gα$_{13}$ QL (Fig. 1*B*). However, both the T274E and N278A mutations decreased Rho activation by ~50%, and Rho activity could be reduced to nearly basal levels by the T274E/N278A double mutation. Immunoblotting of cell lysates demonstrated equal expression levels of the constructs. These data suggested that residues Thr^{274} and Asn^{278}, but not Asn^{270}, are important for the ability of Gα$_{13}$ to stimulate Rho activation in cells.

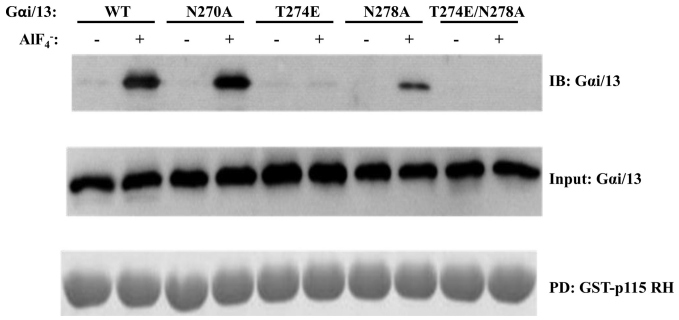

FIGURE 2. **The T274E and N278A mutations impair binding of $G\alpha_{i/13}$ to the RH domain of p115RhoGEF.** $G\alpha_{i/13}$ (wild type or mutant) was incubated with a 50-fold molar excess of GST-p115 RH in the presence or absence of AlF_4^-. GST-p115 RH was pulled down (*PD*) with glutathione-Sepharose beads. Bound proteins were released by boiling and separated by SDS-PAGE. $G\alpha_{i/13}$ was detected by immunoblotting (*IB*). GST-p115 RH was stained with Coomassie Brilliant Blue. Data presented are from one experiment, representative of three independent experiments with similar results.

$G\alpha_{i/13}$ N270A, T274E, N278A, and T274E/N278A Are Functional Gα Subunits—To analyze these mutants in more detail, each mutation was introduced into a construct harboring amino acid residues 1–28 of $G\alpha_{i1}$ and 47–377 of $G\alpha_{13}$ (hereafter referred to as $G\alpha_{i/13}$). The resulting protein was expressed and purified from Sf9 cells for biochemical reconstitution assays. The use of this $G\alpha_{i/13}$ chimera facilitates the production of recombinant protein by increasing the yield from Sf9 cells, and it retains all of the biochemical properties characteristic of native $G\alpha_{13}$, including the ability to regulate RH-RhoGEFs (22). In order to confirm that the mutants were functional Gα subunits, limited trypsin digestion assays were performed. In their inactive, or GDP-bound, form, Gα subunits adopt a conformation that renders them susceptible to digestion by the serine protease trypsin (36). However, in the active form, which can be induced by binding to the reversible activator AlF_4^-, the conformation changes such that the Gα subunit is protected from digestion, largely due to ordering of the α_2 helix in switch II, although trypsin still cleaves the N terminus of the Gα subunit. Thus, the protected species runs at a smaller molecular weight than the native protein. Trypsin digestion assays can therefore be used to determine if a Gα subunit is capable of adopting an activated conformation. As shown in Fig. 1*C*, each $G\alpha_{i/13}$ mutant was protected from tryptic digestion in the presence of AlF_4^-, as evidenced by the existence of the lower molecular weight species, indicating that these mutants were capable of undergoing the activation-dependent conformational changes indicative of a functional Gα subunit.

The T274E and N278A Mutations Disrupt Binding to the RH Domain of p115RhoGEF and Impair GAP Activity—Because these mutations were known to be in the $G\alpha_{13}$-p115RhoGEF RH domain interface (17), the ability of these mutants to interact with the RH domain was assessed using GST pull-down assays, and their capacity to respond to the GAP activity of this domain was determined using single turnover GTPase assays. The activation-dependent interaction between each mutant and the RH domain of p115RhoGEF is shown in Fig. 2. Although the N270A mutation had no apparent effect on the ability of $G\alpha_{i/13}$ to interact with GST-p115 RH, the $G\alpha_{i/13}$ T274E mutant had significantly reduced binding, whereas the N278A mutation produced an intermediate effect. The $G\alpha_{i/13}$ T274E/N278A double mutant had no detectable binding to the RH domain under these conditions.

Previous work has established that the isolated RH domain (amino acids 1–252) of p115RhoGEF is as effective a GAP for $G\alpha_{13}$ as the full-length protein (15). Therefore, GST-p115 RH was also used to examine the effects of these mutations on p115 RH-stimulated GAP activity *in vitro* (Fig. 3). Wild type $G\alpha_{i/13}$ has a measurable rate of basal GTP hydrolysis, which can be markedly increased by the presence of GST-p115 RH (Fig. 3*A*). At 0 °C, 10 nM GST-p115 RH increased the initial velocity of the hydrolysis reaction (V_o) from ~0.08 to ~1.8 fmol/s, or ~22-fold (Fig. 3*F*). $G\alpha_{i/13}$ N270A displayed a very similar rate of RH domain-stimulated hydrolysis (Fig. 3*F*). Consistent with the fact that $G\alpha_{i/13}$ T274E binds the RH domain of p115RhoGEF poorly (Fig. 2), its response to the GAP activity of the RH domain was also significantly impaired. In the presence of the RH domain, GTP hydrolysis by $G\alpha_{i/13}$ T274E was reduced to nearly basal levels (Fig. 3, *C* and *F*). In the case of $G\alpha_{i/13}$ N278A, the reduction in GAP activity in response to the RH domain was ~50% (Fig. 3, *D* and *F*). Like $G\alpha_{i/13}$ T274E, the double mutant, $G\alpha_{i/13}$ T274E/N278A, had a rate of RH-stimulated hydrolysis that was reduced to essentially basal levels (Fig. 3, *E* and *F*). Therefore, the T274E mutation strongly affects the ability of $G\alpha_{i/13}$ to bind the RH domain of p115RhoGEF and respond to its GAP activity, whereas the effect of the N278A mutation was also clear but less pronounced. The N270A mutation had no detectable effect on RH domain binding or GAP activity under the assay conditions used in Figs. 2 and 3.

$G\alpha_{i/13}$ T274E/N278A Cannot Bind to Full-length p115RhoGEF—Next, we assessed the ability of the T274E/N278A double mutant to bind to full-length p115RhoGEF by size exclusion chromatography. As shown in Fig. 4, upon activation with AlF_4^-, $G\alpha_{i/13}$ forms a stable complex with p115RhoGEF, as evidenced by its elution in earlier, p115RhoGEF-containing fractions. In contrast, binding of the double mutant to full-length p115RhoGEF in the presence of AlF_4^- was not detectable at the level of Coomassie Brilliant Blue staining. Given that micromolar concentrations of p115RhoGEF and $G\alpha_{i/13}$ T274E/N278A were insufficient to form a stable complex during the course of gel filtration, the affinity of $G\alpha_{i/13}$ T274E/N278A for full-length p115RhoGEF is likely to be quite low, suggesting that the primary binding site for $G\alpha_{13}$ is in the RH domain.

$G\alpha_{13}$ T274E/N278A Fails to Activate p115RhoGEF in Vitro—We next examined whether $G\alpha_{i/13}$ T274E/N278A could regulate p115RhoGEF activity directly by measuring GTPγS binding to RhoA in vitro. Although $G\alpha_{i/13}$ was able to stimulate RhoA activation through p115RhoGEF (Fig. 5*A*), $G\alpha_{i/13}$ T274E/N278A failed to increase GTPγS binding to RhoA over the p115RhoGEF only condition. These results demonstrate that the T274E/N278A double mutation inhibits the ability to $G\alpha_{i/13}$ to stimulate the nucleotide exchange activity of p115RhoGEF.

Recently, we successfully generated recombinant, full-length $G\alpha_{13}$ comprising amino acid residues 2–377. In the course of analyzing this protein, we found that it is a more efficient activator of RhoA *in vitro* than a functionally equivalent amount of $G\alpha_{i/13}$ (Fig. 5*B*). This suggests that the N-terminal region of

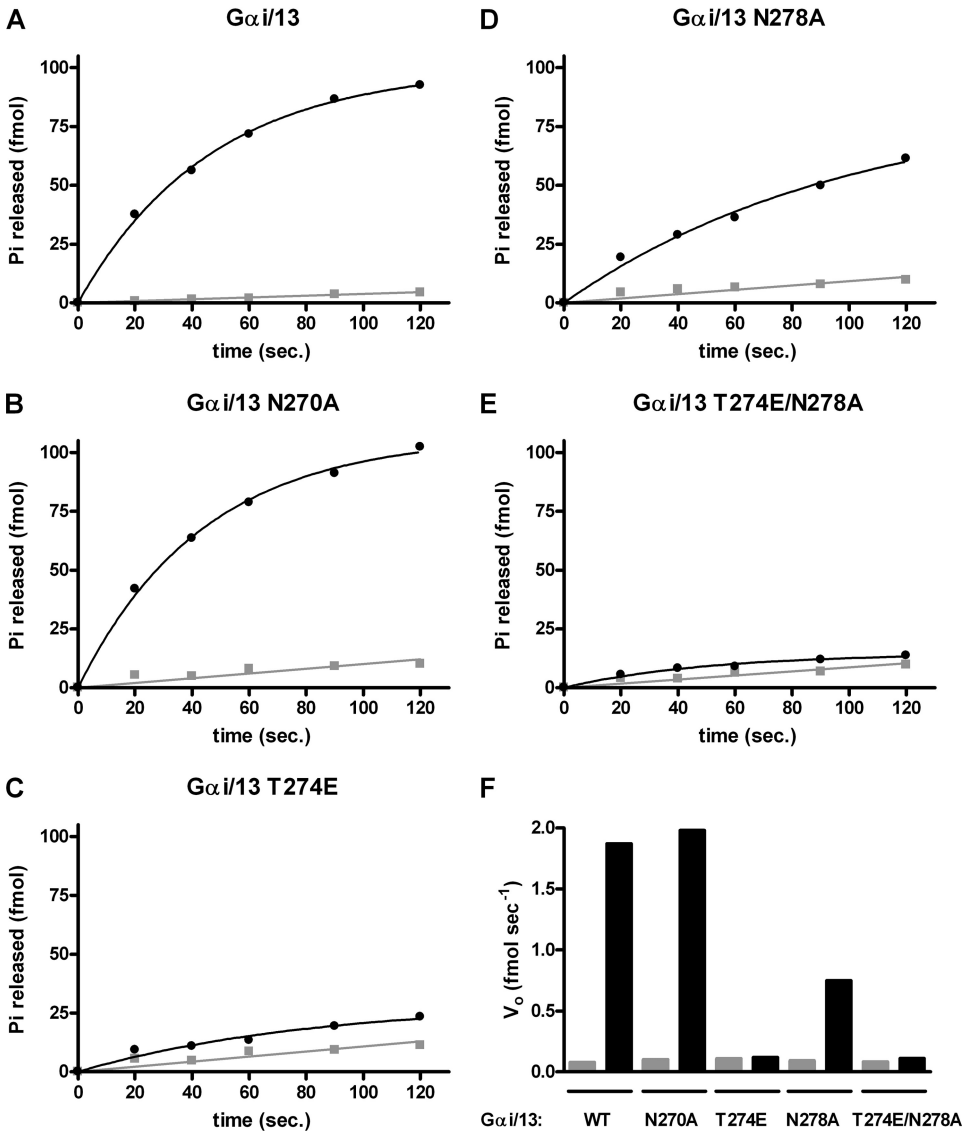

FIGURE 3. **The T274E and N278A mutations in $G\alpha_{i/13}$ impair the GAP response to the RH domain of p115RhoGEF.** *A–E*, $G\alpha_{i/13}$ or the indicated mutant was preloaded with [γ-^{32}P]GTP (final Gα concentration 8–10 nM), and hydrolysis of bound GTP was initiated by mixing with buffer containing 8 mM $MgSO_4$ and 1 mM GTP in the presence (●) or absence (■) of 10 nM GST-p115 RH. Reactions were incubated on ice, and aliquots were removed and quenched in activated charcoal slurry (pH 3) at the indicated times. *F*, the apparent initial rate of GTP hydrolysis by $G\alpha_{i/13}$ or the indicated mutant is shown in the presence (*black bar*) or absence (*gray bar*) of 10 nM GST-p115 RH. Data presented are from one experiment representative of three independent experiments with similar results.

$G\alpha_{13}$ may play a role in efficient stimulation of RhoGEF activity. Due to the higher activity of $G\alpha_{13}$ in the *in vitro* RhoGEF assay, we chose to confirm the effect of the T274E/N278A mutations in the background of this full-length protein and examined its ability to stimulate RhoGEF activity. 100 nM full-length $G\alpha_{13}$ was able to significantly increase the amount of GTPγS bound to RhoA compared with the p115RhoGEF only condition (Fig. 5, *B* and *C*). In contrast, RhoA activation stimulated by a functionally equivalent amount of $G\alpha_{13}$ T274E/N278A was significantly reduced compared with wild type $G\alpha_{13}$ (Fig. 5*C*). The effects of the T274E and N278A mutations on the ability of $G\alpha_{13}$ to stimulate p115RhoGEF activity *in vitro* are shown in supplemental Fig. 1. We note that in contrast to the SRE assay, in which the activity of both $G\alpha_{13}$ QL T274E and $G\alpha_{13}$ QL N278A was reduced ~50% (Fig. 1*B*), $G\alpha_{13}$ T274E failed to stimulate RhoA activation *in vitro*, whereas $G\alpha_{13}$ N278A had no apparent defect. However, *in vitro*, the functional concentration of $G\alpha_{13}$ and its mutants was quantitated by [^{35}S]GTPγS binding, which allows for a comparison between functionally equivalent amounts of protein. In contrast, the SRE assay is a cell-based overexpression system that precludes the tight control over the concentration of $G\alpha_{13}$ afforded by our reconstitution assay. Thus, it is difficult to make a direct comparison between the behavior of the mutants *in vitro* and in cell-based experiments. Taken together, the results using both $G\alpha_{i/13}$ and $G\alpha_{13}$ are consistent and in agreement with the results of the cell-based assays, thus providing strong evidence that residues in the α_3 helix of $G\alpha_{13}$ regulate the GEF activity of p115RhoGEF.

X-ray Crystallography of the $G\alpha_{i/13}$-p115RhoGEF RH Domain Complex—To gain more insight into the interaction between $G\alpha_{i/13}$ and p115RhoGEF, we purified the ternary complex of $G\alpha_{i/13}$, a deletion mutant of p115RhoGEF lacking the region C-terminal to the PH domain (p115RhoGEFΔC), and

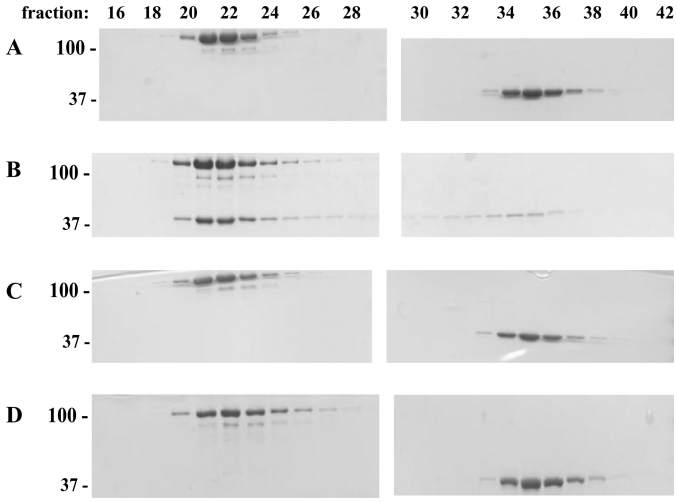

FIGURE 4. **The T274E/N278A double mutation in $G\alpha_{i/13}$ impairs binding to full-length p115RhoGEF.** p115RhoGEF was incubated with $G\alpha_{i/13}$ and GDP (*A*), $G\alpha_{i/13}$ and AlF_4^- (*B*), $G\alpha_{i/13}$ T274E/N278A and GDP (*C*), or $G\alpha_{i/13}$ T274E/N278A and AlF_4^- (*D*). The molar ratio of $G\alpha_{i/13}$ (wild type or mutant) to p115RhoGEF was 2:1. Proteins were fractionated on a Superdex 200 size exclusion column, separated by SDS-PAGE, and stained with Coomassie Brilliant Blue. Fraction numbers are indicated. The positions of molecular mass standards, in kDa, are shown on the *left*.

RhoA by size exclusion chromatography in the presence of AlF_4^- and subjected the complex to crystallization screening. Platelike crystals formed at 20 °C after ~6 weeks and contained a complex of $G\alpha_{i/13}$ and the RH domain of p115RhoGEF. However, the region C-terminal to the RH domain, including the DH and PH domains and RhoA, was not present in the crystal. The x-ray crystal structure of the p115RhoGEF RH domain in complex with $G\alpha_{i/13}$, GDP, Mg^{2+}, and AlF_4^- was determined at 2.4 Å resolution (Table 1). The structure contained two pairs of the $G\alpha_{i/13}$-p115RhoGEF RH domain complex in the asymmetric unit (A-B and C-D; molecules A and C designate $G\alpha_{i/13}$, and molecules C and D designate the p115RhoGEF RH domain (see supplemental Tables 1 and 2)). The final model contains residues 47–336 and 341–372 of molecule A; residues 22–34, 46–85, 93–121, and 134–233 of molecule B; residues 47–336 and 341–368 of molecule C; residues 22–32, 46–85, 92–115, 138–176, and 183–233 of molecule D; 2 GDP; 2 Mg^{2+}; 2 AlF_4^-; and 87 water molecules. For the purpose of discussing the crystal structure, we hereafter refer to the complex as $G\alpha_{13}$-p115 RH because the N terminus of $G\alpha_{i/13}$ containing the residues from $G\alpha_{i1}$ was disordered, and thus, only residues native to $G\alpha_{13}$ were present.

Overall Structure—In general, the structure of the $G\alpha_{13}$-p115 RH complex is similar to the previously reported crystal structure of the $G\alpha_{13/i1}$ chimera-p115RhoGEF RH domain complex (17). Both $G\alpha_{13/i1}$ and $G\alpha_{13}$ interact with the RH domain of p115RhoGEF through two distinct surfaces (Fig. 6). The N-terminal extension of the RH domain, the βN-αN hairpin, makes extensive contacts with the helical domain and switch regions I and II of $G\alpha_{13/i1}$. This interface is also present in the current structure; however, the βN strand is disordered (Fig. 6). Additionally, the RGS box binds to an effector-like interaction surface consisting of the α_2 and α_3 helices and α_3-β_5 loop of both $G\alpha_{13/i1}$ and $G\alpha_{i/13}$ (Fig. 6). However, unlike the $G\alpha_{i/13}$ used in the current study, $G\alpha_{13/i1}$ contains several residues from $G\alpha_{i1}$ in its effector interface, and its ability to stimulate RhoGEF activity has not been clearly demonstrated. The result of these substitutions is a significant difference in the effector interfaces between the two structures at the atomic level.

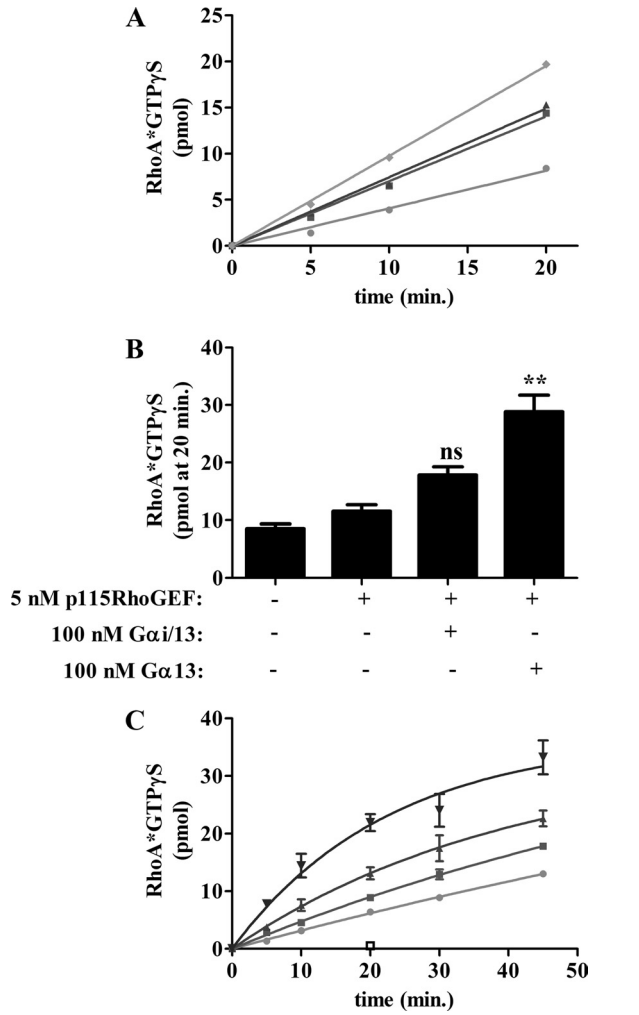

FIGURE 5. **Analysis of RhoA activation *in vitro*.** GTPγS binding to RhoA (final concentration 500 nM) was measured in the presence of buffer, 5 nM p115RhoGEF, or 5 nM p115RhoGEF and 100 nM of the indicated AlF_4^--activated Gα subunit. Samples were incubated at 30 °C and quenched in ice-cold buffer containing 10 mM $MgSO_4$ at the indicated time. *A*, $G\alpha_{i/13}$ T274E/N278A fails to stimulate p115RhoGEF activity *in vitro*. Samples are as follows: RhoA only (●), p115RhoGEF (■), p115RhoGEF plus $G\alpha_{i/13}$ T274E/N278A (▲), and p115RhoGEF plus $G\alpha_{i/13}$ (◆). Data are presented as the mean of single determinations pooled from two independent experiments. *B*, full-length $G\alpha_{13}$ is a more efficacious activator of p115RhoGEF *in vitro* than $G\alpha_{i/13}$. GTPγS binding to RhoA was determined after a 20-min incubation as described above. Data are presented as the mean ± S.E. (*error bars*) of single determinations pooled from three independent experiments. Data were analyzed by one-way analysis of variance, followed by Dunnett's post-test. Statistically significant difference from the p115RhoGEF condition is shown as follows. *ns*, not significant; **, $p < 0.01$. *C*, the T274E/N278A double mutation significantly reduces p115RhoGEF activation by full-length $G\alpha_{13}$. Samples are as follows: RhoA only (●), p115RhoGEF (■), p115 RhoGEF plus $G\alpha_{13}$ T274E/N278A (▼), p115RhoGEF plus $G\alpha_{13}$ (▲), and $G\alpha_{13}$ alone (□). Data are presented as the mean ± S.E. of single determinations pooled from three independent experiments.

The Effector Interface—Compared with $G\alpha_{13/i1}$, $G\alpha_{13}$ is shifted 3 Å closer to the RH domain of p115RhoGEF. This is probably a reflection of the higher affinity of this domain for $G\alpha_{13}$ *versus* $G\alpha_{13/i1}$. Additionally, the bulky side chain of Trp^{280} in $G\alpha_{13/i1}$, which corresponds to Val^{280} in $G\alpha_{13}$, may sterically

TABLE 1
Crystallography statistics
All numbers in parentheses refer to the highest resolution shell statistics.

Parameters	Values
Data collection	
Space group	P1
Unit cell parameters	a = 50.5 Å, b = 70.6Å, c = 88.1 Å, α = 77.8°, β = 84.5°, γ = 80.1°
Wavelength (Å)	1.0
Resolution range (Å)	50–2.4
Redundancy	1.7
Unique reflections	37,777
Completeness (%)	81.8 (82.1)
$I/\sigma(I)$	9.0 (2.3)
R_{sym} [a]	0.074 (0.296)
Refinement	
Resolution range (Å)	48.88–2.40 (2.49–2.40)
No. of reflections	37,316
R-Factor/Free R-factor [b]	0.205/0.280
No. of protein atoms	8,091
No. of magnesium ion atoms	2
No. of ligand atoms	66
No. of water molecules	87
Root mean square deviations	
Bond lengths (Å)	0.009
Bond angles (degrees)	1.4
Average B-value (Å^2)	51.6

[a] $R_{sym} = \Sigma|I_{avg} - Ii|/\Sigma Ii$, where Ii is the observed intensity and I_{avg} is the average intensity.
[b] Free R-factor is calculated for 10% of randomly selected reflections excluded from refinement.

inhibit the formation of a tight complex. $G\alpha_{13}$ forms more hydrogen bonds with p115 RH as compared with $G\alpha_{13/i1}$ (9 *versus* 3 possible hydrogen bonds) (Fig. 6). In $G\alpha_{13}$, Glu^{273} forms an ion pair with Lys^{160} in the RH domain of p115RhoGEF. In contrast, Glu^{273} in $G\alpha_{13/i1}$ makes no contact with the RH domain, whereas Lys^{160} participates in a van der Waals interaction with Ser^{274} of $G\alpha_{13/i1}$. The backbone of Thr^{274} in $G\alpha_{13}$ (Ser^{274} in $G\alpha_{13/i1}$) engages the side chain of Gln^{69} of the RH domain through hydrogen bonding, whereas $G\alpha_{13/i1}$ interacts with Gln^{69} via a hydrogen bond with the side chain of Asn^{278}. Given that this is one of the three possible hydrogen bonds between $G\alpha_{13/i1}$ and the RH domain of p115RhoGEF, perturbing this interaction might be expected to result in a large decrease in binding. However, the results of our experiments with the N278A mutant of $G\alpha_{13}$ suggest that this residue is not as critical for the interaction with the RH domain of p115RhoGEF as Thr^{274}. Consistent with this notion, in $G\alpha_{13}$, Asn^{278} does not participate in hydrogen bonding to p115 RH but rather is in hydrophobic contact with Leu^{68}. Arg^{279} of $G\alpha_{13}$ makes extensive contacts with p115 RH, including a hydrogen bond to the backbone carboxyl group of Phe^{70}, a residue that has previously been implicated in binding to $G\alpha_{13}$ (14). In contrast, Phe^{70} makes no contact with $G\alpha_{13/i1}$. Additionally, Arg^{279} hydrogen-bonds to two additional residues in the RH domain, Ala^{67} and Leu^{68}, through a main chain-side chain bond and a main chain-main chain bond, respectively. As a result of these amino acid differences, the calculated surface area buried in the effector interface of the $G\alpha_{13}$-p115 RH complex (1,600 Å^2) is significantly larger than that of the $G\alpha_{13/i1}$-p115 RH complex (1,200 Å^2).

The GAP Interface—Although there are significant differences in the effector interface between $G\alpha_{13}$ and $G\alpha_{13/i1}$, both interact with the GAP surface of the RH domain in an essentially identical manner (supplemental Fig. 2), which is consistent with the fact that the α helical domain and switch regions of $G\alpha_{13/i1}$ are largely derived from $G\alpha_{13}$. The interaction between the catalytic residue Arg^{200} of $G\alpha_{13}$ and Glu^{27} of p115 RH is found in both structures. Arg^{260} in $G\alpha_{13/i1}$, which hydrogen-bonds with the main chain carbonyl of Ile^{23} and forms an ion pair with Asp^{28} in p115 RH, participates in the same bonding interactions in the $G\alpha_{13}$-p115 RH structure. Likewise, the interaction between Met^{257} from $G\alpha_{13}$ and Phe^{31} of p115 RH, which in the $G\alpha_{13/i1}$-p115 RH domain structure is a van der Waals contact, is also present in the current structure (supplemental Table 1).

Structural Aspects of the N270A, T274E, and N278A Mutations—In the $G\alpha_{13}$-p115 RH domain complex, Asn^{270} of $G\alpha_{13}$ interacts with p115 RH primarily via hydrophobic contact with Met^{163}. However, this interaction is well outside of the effector interface, supporting the results of cell-based experiments demonstrating that the N270A mutation does not impact GEF activity. In contrast, the T274E mutation resulted in reduced Rho activation in cells and severely disrupted binding to p115 RH and the GAP response. These observations are consistent with the fact that Thr^{274} hydrogen-bonds, via its backbone carbonyl, to Gln^{69} in the p115 RH domain, a residue known to be important for $G\alpha_{13}$ binding (14). It is likely that the introduction of a longer, charged side chain in place of Thr^{274}, as is the case with the T274E mutation, disrupts the interaction with Gln^{69} and that this reduced binding results in impaired GAP and GEF activity. Additionally, in molecules C and D, Thr^{274} in $G\alpha_{13}$ makes additional contacts with p115 RH via hydrogen bonding of its side chain to the side chain of Lys^{160} and hydrophobic interaction with Met^{165}. Thus, the effects of the T274E mutation may also be manifest in the form of steric clashing and perturbation of hydrophobic contacts. To probe the role of the side chain of Thr^{274} in the interaction with the RH domain of p115RhoGEF, we made several additional point mutations at this position in $G\alpha_{13}$ and assessed the activity of these mutants in the SRE assay. As shown in Fig. 7*A*, neither the T274A nor the T274S mutation affected Rho activation by $G\alpha_{13}$ QL in this system. Although the T274V mutant had slightly reduced activity, the effect was not nearly as severe as the T274E mutation. Thus, these data strongly suggest that Thr^{274} interacts with the RH domain primarily through its backbone. Asn^{278} interacts with p115 RH solely through a hydrophobic interaction with residue Leu^{68}. Thus, the modest decreases in binding to the RH domain and GAP activity caused by the N278A mutation are consistent with the fact that Asn^{278} does not contribute substantially to the interface with p115 RH. In addition, other residues in $G\alpha_{13}$ that we did not initially target for site-directed mutagenesis also contribute to the interface with the RH domain of p115RhoGEF, namely Glu^{273} and Arg^{279}. In order to determine if these residues contribute to the ability of $G\alpha_{13}$ to stimulate GEF activity, the E273K and R279E mutants were generated and analyzed by an SRE assay. As shown in Fig. 7*B*, mutation of these residues impairs the ability of $G\alpha_{13}$ to stimulate Rho activation in cells, consistent with the notion that the $G\alpha_{13}$-p115 RH interface has the capacity to regulate effector activity. Thus, the results of the current biochemical analysis as well as previously published mutational analysis of p115RhoGEF (14) are more consistent with the

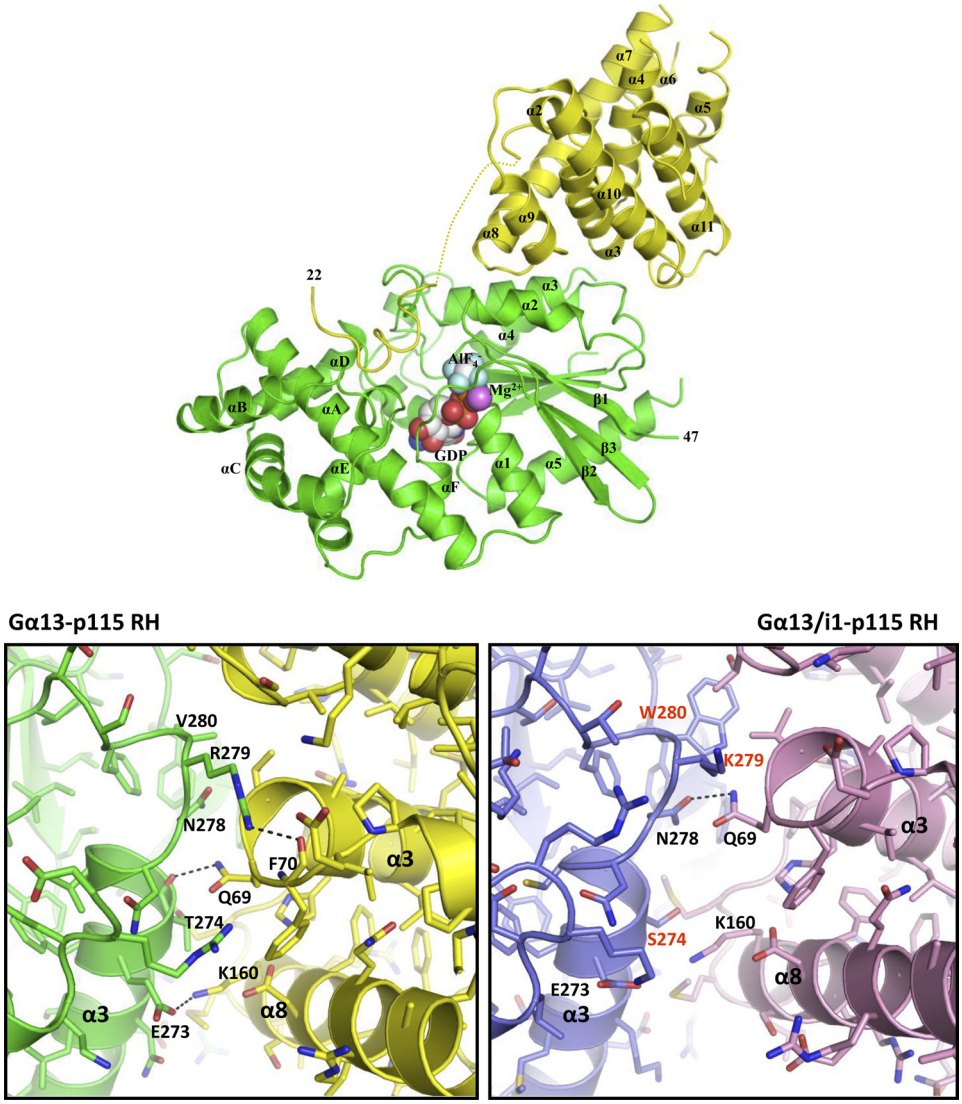

FIGURE 6. **Structure of the $G\alpha_{13}$-p115 RH complex.** *Top*, the $G\alpha_{13}$-p115RhoGEF RH domain complex. The complex is shown as a *ribbon diagram*, with $G\alpha_{13}$ *colored* in *green* and the RH domain of p115RhoGEF in *yellow*. GDP, Mg^{2+}, and AlF_4^- are shown as *space-filling spheres*. Carbon, oxygen, nitrogen, phosphate, magnesium, aluminum, and fluoride atoms are *colored white*, *red*, *dark blue*, *orange*, *purple*, *light gray*, and *light blue*, respectively. The disordered region in p115RhoGEF between the GAP interface and the RGS box is shown as a *dashed yellow line*. *Bottom*, a detailed view of the $G\alpha_{13}$-p115 RH domain effector interface. The $G\alpha_{13}$-p115 RH complex is shown on the *left*, and for comparison, the $G\alpha_{13/i1}$-p115 RH complex (Protein Data Bank entry 1SHZ) is shown on the *right* (17). The former is *colored* as in the *top*, whereas in the latter structure, $G\alpha_{13/i1}$ is *colored blue*, and the p115 RH domain is *purple*. Residues that contribute to the Gα-p115 RH interface are labeled. In $G\alpha_{13/i1}$, residues that are not native to $G\alpha_{13}$ are indicated in *red*. Hydrogen bonds are depicted as *dashed lines*. Oxygen and nitrogen atoms are *colored red* and *blue*, respectively.

$G\alpha_{13}$-p115 RH interface presented here than with the interface between the RH domain and $G\alpha_{13/i1}$.

Comparison with PDZ-RhoGEF—Interestingly, the effector interface between $G\alpha_{13}$ and the RH domain of p115RhoGEF is largely conserved in PDZ-RhoGEF (Fig. 8 and supplemental Table 3). Although Asn^{270} of $G\alpha_{13}$ participates in hydrophobic interaction with p115 RH, mutation of this residue has no apparent effect on binding, GAP, or GEF activity in cells. There is no interaction between this residue and PDZ-RhoGEF. In contrast, residue Thr^{274} of $G\alpha_{13}$, due to rotation of the side chain, makes more extensive contact with PDZ-RhoGEF RH than with p115RhoGEF RH. In addition to the interaction with Gln^{351}, which is analogous to Gln^{69} in p115RhoGEF, via its backbone carbonyl group, Thr^{274} is also involved in hydrophobic interactions with Lys^{439} and Leu^{444}. Residue Asn^{278} in $G\alpha_{13}$ also interacts with Gln^{351} of PDZ-RhoGEF via hydrophobic contact. Arg^{279} of $G\alpha_{13}$, which has extensive interaction with the RH domain of p115RhoGEF, makes fewer contacts with PDZ-RhoGEF. However, the main chain-main chain interaction between Arg^{279} and Leu^{68} of p115RhoGEF is conserved in the analogous residue of PDZ-RhoGEF, Ser^{350}. Thus, the prominent features of the effector interface between $G\alpha_{13}$ and p115RhoGEF RH are conserved in the $G\alpha_{13}$-PDZ-RhoGEF RH crystal structure as well, suggesting that this interface may also play a role in regulating the GEF activity of PDZ-RhoGEF.

DISCUSSION

The RH domains found in RH-RhoGEFs, such as p115RhoGEF, are characterized by low sequence identity to classical RGS domain-containing proteins, such as RGS2 and

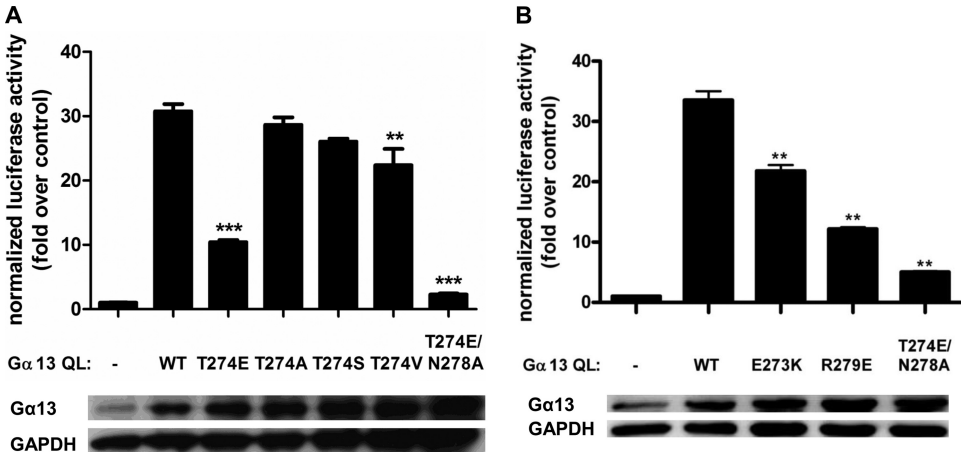

FIGURE 7. **Mutational analysis of the effector interface between $G\alpha_{13}$ and p115 RH.** *A*, the T274A and T274S mutations in $G\alpha_{13}$ fail to impair Rho activation in cells. HeLa cells were transiently transfected with empty vector or the indicated $G\alpha_{13}$ QL construct. The luciferase activity of cell lysates was determined as described under "Experimental Procedures." Total cell lysate was immunoblotted for either $G\alpha_{13}$ or GAPDH. Data are presented as the mean ± S.E. (*error bars*) of triplicate determinations from a single experiment, representative of three independent experiments with similar results. Data were analyzed by one-way analysis of variance followed by Dunnett's post-test. Statistically significant difference from $G\alpha_{13}$ QL is shown as follows. **, $p < 0.01$; ***, $p < 0.001$. *B*, the E273K and R279E mutations in $G\alpha_{13}$ impair Rho activation in cells. Assays were performed as in *A*. Statistically significant difference from $G\alpha_{13}$ QL is shown as follows. **, $p < 0.01$.

RGS4 (12, 37). Additionally, unlike these RGS proteins, the RGS box of p115RhoGEF does not contain the residues necessary to accelerate GTP hydrolysis by $G\alpha_{13}$; these catalytic residues are found in the acidic βN-αN hairpin N-terminal to the RGS box (14, 17). The RH domain of p115RhoGEF has also been implicated in the regulation of nucleotide exchange activity because deletion of the first 288 amino acids of p115RhoGEF impairs both basal and $G\alpha_{13}$-stimulated GEF activity (15). Given that removal of the first 42 amino acids of p115RhoGEF, which are required for GAP activity, has no effect on the ability of $G\alpha_{13}$ to stimulate GEF activity (15), the GAP and GEF functions are clearly distinct properties of the RH domain. However, specific residues in $G\alpha_{13}$ responsible for stimulating p115RhoGEF activity have not been identified. Although x-ray crystallography has demonstrated that a $G\alpha_{13/i1}$ chimera forms a putative effector-like interface with the RH domain of p115RhoGEF (17), the capacity of residues in this interface, many of which are derived from $G\alpha_{i1}$, to regulate GEF activity is unknown.

Our results demonstrate that $G\alpha_{13}$ regulates p115RhoGEF activity via the classical effector interface it forms with the RH domain. Specifically, mutation of Thr^{274} and Asn^{278} in the α_3 helix of $G\alpha_{13}$ impairs the ability of $G\alpha_{13}$ to stimulate Rho activation in cells, impairs binding to p115RhoGEF, and reduces the capacity of $G\alpha_{13}$ to stimulate the guanine nucleotide exchange activity of p115RhoGEF *in vitro*. We also determined the structure of the $G\alpha_{13}$-p115RhoGEF RH complex and found that this effector interface differs in several important respects from the interface formed with $G\alpha_{13/i1}$. Importantly, these new structural data are strongly supported by the results of our biochemical experiments.

In the context of previously reported data, our results are consistent with earlier studies that broadly defined the RhoGEF-activating surface of $G\alpha_{13}$ as the region C-terminal to the Ras-like domain (32), more specifically the last 100 amino acid residues (23). However, given that we have demonstrated that the interaction between the RH domain and $G\alpha_{13}$ also regulates the effector activity of p115RhoGEF, this suggests that the previously described interface between $G\alpha_{13}$ and the DH/PH domains of p115RhoGEF may not contribute significantly to stimulation of GEF activity (15). If the RH domain represents the sole binding site for $G\alpha_{13}$, how might this interaction regulate the activity of the DH/PH domains? One study using PDZ-RhoGEF has suggested that the RH domain may work in concert with elements found in the linker region between the RH and DH domains to regulate GEF activity (38). Specifically, an acidic cluster of residues located in the linker may interact directly with residues in the DH domain to autoinhibit PDZ-RhoGEF activity. Mutation of these residues enhances GEF activity *in vitro* but only in the absence of the RH domain. Recently, the linker between the RH and DH domains of p115RhoGEF has also been implicated in regulating basal GEF activity, although the mechanism of autoinhibition appears to be distinct from that employed by PDZ-RhoGEF (39). A stretch of 40 amino acids located in the linker region of p115RhoGEF has been proposed to disrupt the interaction between the DH domain and residues in the "GEF switch" immediately N-terminal to it, an interaction that is critical for basal GEF activity. Thus, one consequence of $G\alpha_{13}$ binding to the RH domain may be to reorient elements within the linker region of these RH-RhoGEFs, allowing for enhanced exchange activity.

A comparison of the structures of $G\alpha_{13}$ bound to the RH domains of p115RhoGEF and PDZ-RhoGEF reveals that it binds this domain in a nearly identical manner. Additionally, the T274E and N278A mutations in $G\alpha_{13}$ also impair the interaction with the RH domain of LARG *in vitro* (data not shown). Thus, it is likely that $G\alpha_{13}$ engages the RH domains of all three RH-RhoGEFs in the same manner and stimulates RhoGEF activity through a similar mechanism. Although LARG is clearly regulated directly by $G\alpha_{13}$ *in vitro* (40), stimulation of the RhoGEF activity of PDZ-RhoGEF by $G\alpha_{13}$ *in vitro* has not been detectable under the conditions tested (15). However, PDZ-RhoGEF has been linked to $G\alpha_{13}$-mediated Rho activation in cells (10). Thus, although the effector interface formed between $G\alpha_{13}$ and the RH domain of p115RhoGEF bears strik-

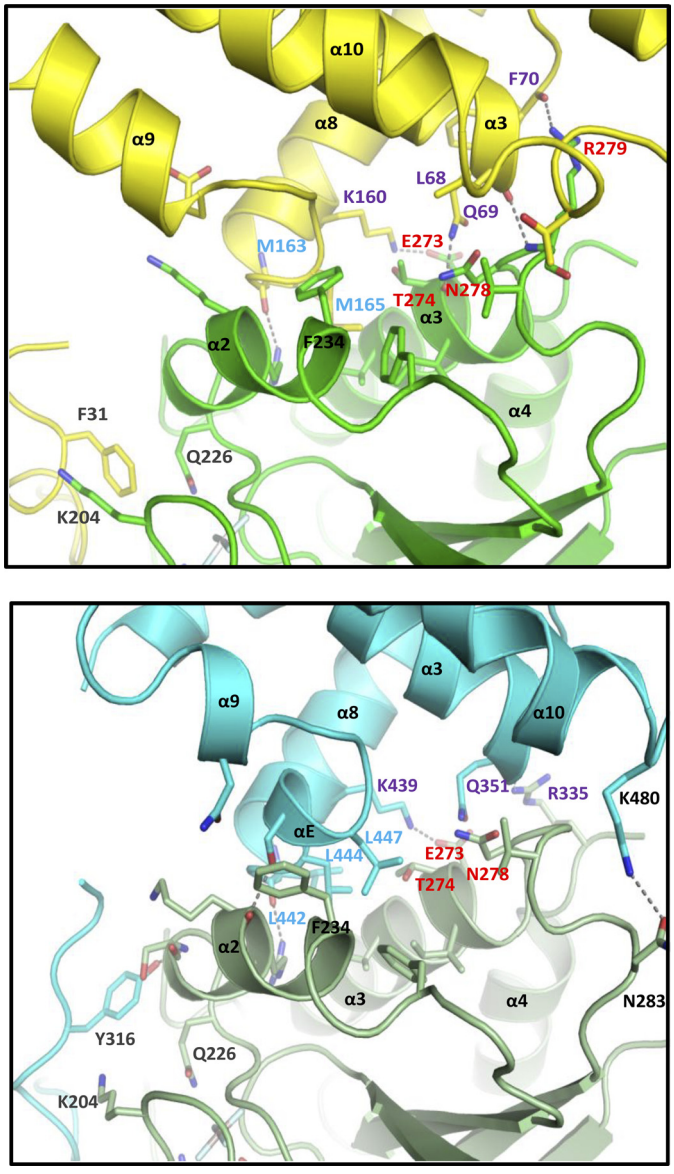

FIGURE 8. **Comparison of the interaction between $G\alpha_{13}$ and the RH domains of p115RhoGEF and PDZ-RhoGEF.** *Top*, the effector interface formed by $G\alpha_{13}$ and the RH domain of p115RhoGEF. The interface is depicted as a *ribbon diagram*, with $G\alpha_{13}$ colored in *green* and the RH domain in *yellow*. Oxygen and nitrogen atoms are *colored red* and *blue*, respectively. Hydrogen bonds are depicted as *dashed lines*. Residues that contribute to the GAP interface are labeled in *gray*, whereas hydrophobic residues that contribute to the effector interface by the RH domain are labeled in *light blue*. Residues in $G\alpha_{13}$ that affect its capacity to stimulate the GEF activity of p115RhoGEF are labeled in *red*, and their bonding partners in the RH domain are labeled in *purple*. The conformationally flexible residue Phe^{234} in $G\alpha_{13}$ is labeled in *black*. *Bottom*, the effector interface formed by $G\alpha_{13}$ and the RH domain of PDZ-RhoGEF (Protein Data Bank entry 3CX7) (45). The interface is depicted as a *ribbon diagram*, with $G\alpha_{13}$ colored in *olive green* and the RH domain in *light blue*. Atoms and amino acid residues are labeled as in the *top*.

ing resemblance to the $G\alpha_{13}$-PDZ-RhoGEF RH interface, in the latter case, this interaction is not sufficient to regulate RhoGEF activity *in vitro*. Post-translational modification, such as phosphorylation, or interaction with a co-activating protein may be required to render PDZ-RhoGEF susceptible to regulation by $G\alpha_{13}$.

It is also possible that activation of p115RhoGEF by $G\alpha_{13}$ requires multiple intermolecular interfaces. Binding of $G\alpha_{13}$ to the RH domain may result in a conformational change that brings additional regions of p115RhoGEF, perhaps the catalytic DH/PH domains, into contact with $G\alpha_{13}$, allowing for efficient activation of exchange activity. Although activated $G\alpha_{13}$ clearly fails to stimulate the GEF activity of p115RhoGEF fragments lacking the RH domain, it has been reported to bind to the isolated DH/PH domains of p115RhoGEF *in vitro* (15). Additionally, the N terminus of $G\alpha_{13}$, which is replaced by the αN helix of $G\alpha_{i1}$ in $G\alpha_{i/13}$ and is disordered in the present crystal structure, may contribute to the binding interface with p115RhoGEF. This hypothesis is supported by the fact that $G\alpha_{13}$ exhibits more robust activity in the RhoGEF assay compared with $G\alpha_{i/13}$ *in vitro* (Fig. 5*B*). The results of our gel filtration analysis suggest that $G\alpha_{i/13}$ T274E/N278A cannot bind to p115RhoGEF and are consistent with the *in vitro* RhoGEF assays demonstrating that $G\alpha_{i/13}$ T274E/N278A fails to stimulate RhoA activation over the p115RhoGEF condition. These data argue in favor of a model in which $G\alpha_{13}$ binds exclusively to the RH domain; however, it is difficult to rule out the possibility of additional low affinity binding sites outside of the RH domain. Given that the RH domain occupies the classical effector interface on $G\alpha_{13}$, any additional interface would probably be a novel surface that has not been observed in other $G\alpha$-effector pairs. Aside from the residues reported here, however, screening of additional $G\alpha_{13}$ mutants has so far failed to identify other residues that affect its capacity to stimulate Rho activation in cells.[4]

Little is known about the mechanism by which the other G_{12} family member, $G\alpha_{12}$, stimulates RH-RhoGEF activity. p115RhoGEF also functions as a GAP for $G\alpha_{12}$ and serves as an effector in cells; however, $G\alpha_{12}$ is incapable of activating p115RhoGEF *in vitro* (9). Because $G\alpha_{12}$ and $G\alpha_{13}$ have a high degree of identity at the primary sequence level (~69%) and have nearly identical α_3 helices and α_3-β_5 loops, it is worthwhile to consider biochemically whether $G\alpha_{12}$ and $G\alpha_{13}$ bind to the RH domain of p115RhoGEF using the same interface. When mutations corresponding to the $G\alpha_{13}$ mutants described here were introduced into $G\alpha_{12}$, the pattern of Rho activation in SRE assays and binding to the RH domain of p115RhoGEF was similar to that observed with the $G\alpha_{13}$ mutants (supplemental Fig. 3). This suggests that the binding site for $G\alpha_{12}$ overlaps with that of $G\alpha_{13}$ in the RH domain of p115RhoGEF and probably explains the observation that activated $G\alpha_{12}$ can inhibit $G\alpha_{13}$-mediated activation of p115RhoGEF despite the fact that $G\alpha_{12}$ cannot directly activate p115RhoGEF *in vitro* (9). However, these data imply that the inability of $G\alpha_{12}$ to stimulate p115RhoGEF is not due to a difference in primary sequence, as had previously been suggested (23). Thus, the reasons behind this lack of activity remain unknown. However, as another RH-RhoGEF, LARG, needs to be tyrosine-phosphorylated in order to be responsive to $G\alpha_{12}$ *in vitro* (40), this may be the case with p115RhoGEF as well.

Although the precise activation mechanism of p115RhoGEF remains to be fully elucidated, we have identified residues in $G\alpha_{13}$ that play a role in regulating the nucleotide exchange

[4] N. Hajicek and T. Kozasa, unpublished data.

activity of p115RhoGEF. However, given that p115RhoGEF activity is also reported to be regulated by subcellular localization (41–43) and post-translational modification (44), the activation mechanism in cells is likely to be complex. Ongoing efforts to crystallize $G\alpha_{13}$ and $G\alpha_{12}$ with p115RhoGEF constructs containing the RH domain and DH/PH domains will aid in directly addressing the presence of additional binding sites and will help to clarify the molecular mechanism by which heterotrimeric G proteins stimulate activation of this RhoGEF.

Acknowledgments—We are grateful to Dr. John Tesmer for critical reading of the manuscript. We thank Hideko Wakasugi-Masuho, Ami Vora, Terry Phonxanasinh, Dara Chanthavong, Dr. Takashi Umehara, Dr. Kazushige Katsura, Yumiko Terazawa, Takako Fujimoto, and Dr. Motoaki Wakiyama for technical assistance.

REFERENCES

1. Oldham, W. M., and Hamm, H. E. (2006) *Q. Rev. Biophys.* **39,** 117–166
2. Hollinger, S., and Hepler, J. R. (2002) *Pharmacol. Rev.* **54,** 527–559
3. Berman, D. M., Kozasa, T., and Gilman, A. G. (1996) *J. Biol. Chem.* **271,** 27209–27212
4. Tesmer, J. J., Berman, D. M., Gilman, A. G., and Sprang, S. R. (1997) *Cell* **89,** 251–261
5. Strathmann, M. P., and Simon, M. I. (1991) *Proc. Natl. Acad. Sci. U.S.A.* **88,** 5582–5586
6. Mao, J., Yuan, H., Xie, W., Simon, M. I., and Wu, D. (1998) *J. Biol. Chem.* **273,** 27118–27123
7. Lin, F., Chen, S., Sepich, D. S., Panizzi, J. R., Clendenon, S. G., Marrs, J. A., Hamm, H. E., and Solnica-Krezel, L. (2009) *J. Cell Biol.* **184,** 909–921
8. Buhl, A. M., Johnson, N. L., Dhanasekaran, N., and Johnson, G. L. (1995) *J. Biol. Chem.* **270,** 24631–24634
9. Hart, M. J., Jiang, X., Kozasa, T., Roscoe, W., Singer, W. D., Gilman, A. G., Sternweis, P. C., and Bollag, G. (1998) *Science* **280,** 2112–2114
10. Fukuhara, S., Murga, C., Zohar, M., Igishi, T., and Gutkind, J. S. (1999) *J. Biol. Chem.* **274,** 5868–5879
11. Kourlas, P. J., Strout, M. P., Becknell, B., Veronese, M. L., Croce, C. M., Theil, K. S., Krahe, R., Ruutu, T., Knuutila, S., Bloomfield, C. D., and Caligiuri, M. A. (2000) *Proc. Natl. Acad. Sci. U.S.A.* **97,** 2145–2150
12. Kozasa, T., Jiang, X., Hart, M. J., Sternweis, P. M., Singer, W. D., Gilman, A. G., Bollag, G., and Sternweis, P. C. (1998) *Science* **280,** 2109–2111
13. Chen, Z., Wells, C. D., Sternweis, P. C., and Sprang, S. R. (2001) *Nat. Struct. Biol.* **8,** 805–809
14. Chen, Z., Singer, W. D., Wells, C. D., Sprang, S. R., and Sternweis, P. C. (2003) *J. Biol. Chem.* **278,** 9912–9919
15. Wells, C. D., Liu, M. Y., Jackson, M., Gutowski, S., Sternweis, P. M., Rothstein, J. D., Kozasa, T., and Sternweis, P. C. (2002) *J. Biol. Chem.* **277,** 1174–1181
16. Mao, J., Yuan, H., Xie, W., and Wu, D. (1998) *Proc. Natl. Acad. Sci. U.S.A.* **95,** 12973–12976
17. Chen, Z., Singer, W. D., Sternweis, P. C., and Sprang, S. R. (2005) *Nat. Struct. Mol. Biol.* **12,** 191–197
18. Tesmer, J. J., Sunahara, R. K., Gilman, A. G., and Sprang, S. R. (1997) *Science* **278,** 1907–1916
19. Slep, K. C., Kercher, M. A., He, W., Cowan, C. W., Wensel, T. G., and Sigler, P. B. (2001) *Nature* **409,** 1071–1077
20. Tesmer, V. M., Kawano, T., Shankaranarayanan, A., Kozasa, T., and Tesmer, J. J. (2005) *Science* **310,** 1686–1690
21. Lutz, S., Shankaranarayanan, A., Coco, C., Ridilla, M., Nance, M. R., Vettel, C., Baltus, D., Evelyn, C. R., Neubig, R. R., Wieland, T., and Tesmer, J. J. (2007) *Science* **318,** 1923–1927
22. Kreutz, B., Yau, D. M., Nance, M. R., Tanabe, S., Tesmer, J. J., and Kozasa, T. (2006) *Biochemistry* **45,** 167–174
23. Kreutz, B., Hajicek, N., Yau, D. M., Nakamura, S., and Kozasa, T. (2007) *Cell. Signal.* **19,** 1681–1689
24. Singer, W. D., Miller, R. T., and Sternweis, P. C. (1994) *J. Biol. Chem.* **269,** 19796–19802
25. Tanabe, S., Kreutz, B., Suzuki, N., and Kozasa, T. (2004) *Methods Enzymol.* **390,** 285–294
26. Otwinowski, Z., and Minor, W. (1997) *Methods Enzymol.* **276,** 307–326
27. Jones, T. A., Zou, J. Y., Cowan, S. W., and Kjeldgaard, M. (1991) *Acta Crystallogr. A* **47,** 110–119
28. Brünger, A. T., Adams, P. D., Clore, G. M., DeLano, W. L., Gros, P., Grosse-Kunstleve, R. W., Jiang, J. S., Kuszewski, J., Nilges, M., Pannu, N. S., Read, R. J., Rice, L. M., Simonson, T., and Warren, G. L. (1998) *Acta Crystallogr. D Biol. Crystallogr.* **54,** 905–921
29. Collaborative Computational Project No. 4 (1994) *Acta Crystallogr. D Biol. Crystallogr.* **50,** 760–763
30. Holm, L., and Sander, C. (1993) *J. Mol. Biol.* **233,** 123–138
31. DeLano, W. L. (2010) *The PyMOL Molecular Graphics System*, Version 1.3r1, Schrodinger, LLC, New York
32. Vázquez-Prado, J., Miyazaki, H., Castellone, M. D., Teramoto, H., and Gutkind, J. S. (2004) *J. Biol. Chem.* **279,** 54283–54290
33. Waldo, G. L., Ricks, T. K., Hicks, S. N., Cheever, M. L., Kawano, T., Tsuboi, K., Wang, X., Montell, C., Kozasa, T., Sondek, J., and Harden, T. K. (2010) *Science* **330,** 974–980
34. Berstein, G., Blank, J. L., Jhon, D. Y., Exton, J. H., Rhee, S. G., and Ross, E. M. (1992) *Cell* **70,** 411–418
35. Smrcka, A. V., Hepler, J. R., Brown, K. O., and Sternweis, P. C. (1991) *Science* **251,** 804–807
36. Fung, B. K., and Nash, C. R. (1983) *J. Biol. Chem.* **258,** 10503–10510
37. Tesmer, J. J. (2009) *Prog. Mol. Biol. Transl. Sci.* **86,** 75–113
38. Zheng, M., Cierpicki, T., Momotani, K., Artamonov, M. V., Derewenda, U., Bushweller, J. H., Somlyo, A. V., and Derewenda, Z. S. (2009) *BMC Struct. Biol.* **9,** 36
39. Chen, Z., Guo, L., Sprang, S. R., and Sternweis, P. C. (2011) *Protein Sci.* **20,** 107–117
40. Suzuki, N., Nakamura, S., Mano, H., and Kozasa, T. (2003) *Proc. Natl. Acad. Sci. U.S.A.* **100,** 733–738
41. Wells, C. D., Gutowski, S., Bollag, G., and Sternweis, P. C. (2001) *J. Biol. Chem.* **276,** 28897–28905
42. Bhattacharyya, R., and Wedegaertner, P. B. (2003) *Biochem. J.* **371,** 709–720
43. Bhattacharyya, R., and Wedegaertner, P. B. (2000) *J. Biol. Chem.* **275,** 14992–14999
44. Holinstat, M., Mehta, D., Kozasa, T., Minshall, R. D., and Malik, A. B. (2003) *J. Biol. Chem.* **278,** 28793–28798
45. Chen, Z., Singer, W. D., Danesh, S. M., Sternweis, P. C., and Sprang, S. R. (2008) *Structure* **16,** 1532–1543